European Journal of Pharmaceutics and Biopharmaceutics 77 (2011) 89–98

Contents lists available at ScienceDirect

European Journal of Pharmaceutics and Biopharmaceutics

journal homepage: www.elsevier.com/locate/ejpb

Research paper

Incorporation of a synthetic mycobacterial monomycoloyl glycerol analogue stabilizes dimethyldioctadecylammonium liposomes and potentiates their adjuvant effect *in vivo*

Pernille Nordly [a], Karen Smith Korsholm [b], Esra Alici Pedersen [a], Tayba Sajid Khilji [a], Henrik Franzyk [c], Lene Jorgensen [a], Hanne Mørck Nielsen [a], Else Marie Agger [b], Camilla Foged [a,*]

[a] Department of Pharmaceutics and Analytical Chemistry, University of Copenhagen, Copenhagen Ø, Denmark
[b] Department of Infectious Disease Immunology, Vaccine Delivery & Formulation, Statens Serum Institut, Copenhagen S, Denmark
[c] Department of Medicinal Chemistry, University of Copenhagen, Copenhagen Ø, Denmark

ARTICLE INFO

Article history:
Received 1 July 2010
Accepted in revised form 5 October 2010
Available online 20 October 2010

Keywords:
Liposome
Adjuvant
Vaccine
Dimethyldioctadecylammonium
Monomycoloyl glycerol
Nanomedicine

ABSTRACT

The combination of delivery systems such as cationic liposomes and immunopotentiating molecules is a promising approach for the rational design of vaccine adjuvants. In this study, a synthetic analogue of the mycobacterial lipid monomycoloyl glycerol (MMG), referred to as MMG-**1**, was synthesized and combined with the cationic surfactant dimethyldioctadecylammonium (DDA). The purpose of the study was to provide a thorough pharmaceutical characterization of the resulting DDA/MMG-**1** binary system and to evaluate how incorporation of MMG-**1** affected the adjuvant activity of DDA liposomes. Thermal analyses demonstrated that MMG-**1** was incorporated into the DDA lipid bilayers, and cryo-transmission electron microscopy (TEM) confirmed that liposomes were formed. The particles had a polydisperse size distribution and an average diameter of approximately 400 nm. Evaluation of the colloidal stability indicated that at least 18 mol% MMG-**1** was required to stabilize the DDA liposomes as the average particle size remained constant during storage for 6 months. The improved colloidal stability is most likely caused by increased hydration of the lipid bilayer. This was demonstrated by studying Langmuir–Blodgett monolayers of DDA and MMG-**1** which revealed an increased surface pressure in the presence of high concentrations of MMG-**1** when the DDA/MMG-**1** monolayers were fully compressed, indicating an increased interaction with water due to enhanced hydration of the lipid head groups. Finally, immunization of mice with the tuberculosis fusion antigen Ag85B-ESAT-6 and DDA/MMG-**1** liposomes induced a strong cell-mediated immune response characterized by a mixed Th1/Th17 profile and secretion of IgG1 and IgG2c antibodies. The Th1/Th17-biased immunostimulatory effect was increased in an MMG-**1** concentration-dependent manner with maximal observed effect at 31 mol% MMG-**1**. Thus, incorporation of 31 mol% MMG-**1** into DDA liposomes results in an adjuvant system with favorable physical as well as immunological properties.

1. Introduction

The development of subunit vaccines represents a significant improvement in the safety of modern vaccines as these are composed of well-defined and highly pure components. Since protein-based antigens in general are weakly immunogenic by themselves, co-administration of adjuvants is required to induce potent and persistent specific immune responses [1,2]. An example of a compound with adjuvant activity is the quaternary ammonium salt dimethyldioctadecylammonium (DDA) bromide [3] which has been tested in combination with a variety of antigens in experimental animal models [4–7]. DDA is a synthetic surfactant consisting of a hydrophilic, cationic quaternary ammonium head group, and two hydrophobic saturated C_{18} alkyl chains (Fig. 1A). Due to their surfactant properties, DDA molecules self-assemble into liposome-like structures upon dispersion in aqueous media, but the relatively small size and low water-binding capacity of the quaternary ammonium head group render DDA liposomes

Abbreviations: APC, antigen-presenting cell; DDA, dimethyldioctadecylammonium; DSC, differential scanning calorimetry; IFN-γ, interferon γ; IL, interleukin; MMG, monomycoloyl glycerol; PDI, polydispersity index; TDB, trehalose 6,6′-dibehenate; TEM, transmission electron microscopy.

* Corresponding author. University of Copenhagen, The Faculty of Pharmaceutical Sciences, Department of Pharmaceutics and Analytical Chemistry, Universitetsparken 2, DK-2100 Copenhagen Ø, Denmark. Tel.: +45 35 33 64 02.
E-mail address: cfo@farma.ku.dk (C. Foged).

0939-6411/$ - see front matter © 2010 Elsevier B.V. All rights reserved.
doi:10.1016/j.ejpb.2010.10.001

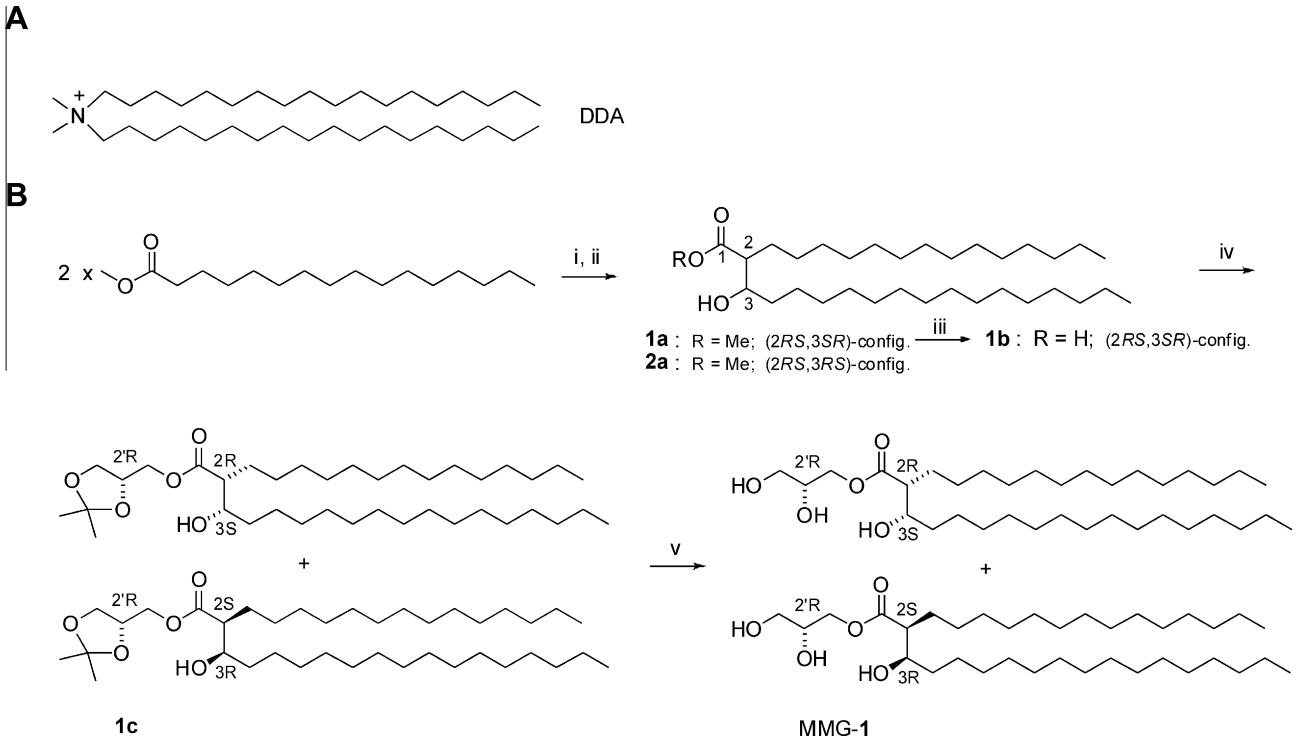

Fig. 1. (A) Molecular structure of dimethyldioctadecylammonium (DDA). (B) Synthesis of MMG-**1**: (i) NaH, dry xylene, reflux, 4 h; (ii) $NaBH_4$, $CHCl_3$–MeOH, 1 h; (iii) 5% KOH, EtOH, 75 °C, 3.5 h; (iv) DCC, HOAt, DMAP, dry CH_2Cl_2, room temperature, 16 h; (v) TFA–THF–H_2O (8:17:3), room temperature, 3.5 h. MMG-**1** consists of two diastereomers with (2*R*, 3*S*, 2′*R*)- and (2*S*, 3*R*, 2′*R)* configuration, respectively. The stereochemistry of the natural MMG corresponds to the (2*R*, 3*R*, 2′*S*)-configuration.

physically unstable resulting in aggregation or flocculation [8–10]. DDA liposomes are therefore pharmaceutically unacceptable as vaccine adjuvants.

Several approaches are commonly applied to stabilize liposomes. These include, among others, grafting of hydrophilic polymers like polyethyleneglycol to the head groups of the lipids and bilayer modification by the introduction of lipids with a higher propensity to interact with the surrounding aqueous medium. An example of the latter is the stabilization of DDA liposomes by incorporation of the glycolipid trehalose 6,6′-dibehenate (TDB) into the liposomal bilayers [9]. The trehalose head groups enable the formation of stabilizing hydrogen bonds between the water molecules in the surrounding aqueous phase and the liposomes [11]. In addition, TDB is a strong immunopotentiator and DDA/TDB liposomes (designated CAF01) have been extensively evaluated in pre-clinical studies showing promising adjuvant activity for subunit vaccines against a wide range of diseases [12] and has recently entered a phase I clinical trial with the tuberculosis fusion antigen Ag85B-ESAT-6 [13,14].

Several components from the mycobacterial cell wall possess immunostimulatory activity [15,16] and membrane lipids extracted from the cell wall of *Mycobacterium bovis* bacillus Calmette-Guérin (*M. bovis* BCG) comprise both polar and apolar lipids with adjuvant activity when co-administered with cationic DDA liposomes [17]. The majority of the adjuvant activity has been attributed to the apolar lipids, especially the lipid monomycoloyl glycerol (MMG) [18,19]. Furthermore, a simple C_{32} lipid-based synthetic analogue of MMG (denoted C_{32} MMG) was demonstrated to possess similar immunological activity upon dispersion with DDA [19].

In the present study, another synthetic MMG analogue of similar chain length (termed MMG-**1**) was investigated. MMG-**1** contains a glycerol head group and two hydrophobic saturated C_{14} and C_{15} alkyl chains, respectively, linked via an ester bond to the glycerol moiety (Fig. 1B). Despite the promising adjuvant activity of MMG, the knowledge about the biophysical and pharmaceutical properties of MMG-containing adjuvants is limited. The present study provides a thorough pharmaceutical characterization of DDA/MMG-**1** liposomes. It is demonstrated that MMG-**1** increases the colloidal stability of DDA liposomes by enabling hydrogen bond formation between the liposomal head groups and the surrounding aqueous solvent. In addition, MMG-**1** potentiates the adjuvant efficacy of DDA liposomes in *in vivo* experiments in mice.

2. Materials and methods

2.1. Materials

Dimethyldioctadecylammonium bromide was obtained from Avanti Polar Lipids (Alabaster, AL, USA). All other chemicals and reagents were obtained commercially at analytical grade.

2.2. Synthesis of MMG-*1*

MMG-**1** was synthesized by a modification of a previously reported pathway [18–20] as described below and in Fig. 1B. The identity of the resulting compounds was confirmed by NMR (see Supplementary data for details of NMR data).

2.2.1. Preparation of (2RS,3SR)- and (2RS,3RS)-corynomycolic acid methyl esters (*1a* and *2a*)

Methyl palmitate (10.67 g, 39.45 mmol) was dissolved in dry *o*-xylene (30 ml), and then NaH (2.08 g, 52 mmol; 60% oil suspension) was added. The mixture was heated to reflux (147 °C bath temperature) for 4 h. Upon cooling to room temperature, HOAc (6 ml, acidic pH) and $CHCl_3$ (200 ml) were added. The resulting mixture was then washed with water (3 × 100 ml), dried (Na_2SO_4),

concentrated (at ca. 55 °C), and then freeze-dried overnight. The crude product (10.87 g) was dissolved in $CHCl_3$–MeOH (1:1, 200 ml), and then $NaBH_4$ (0.75 g, 19.82 mmol) was added in small aliquots under stirring. After 1 h, $CHCl_3$ (300 ml) and water (150 ml) were added. The aqueous layer was extracted with additional $CHCl_3$ (300 ml); the combined organic phases were dried (Na_2SO_4) and concentrated *in vacuo*. The residue was dissolved in CH_2Cl_2–$CHCl_3$ (1:1, 50 ml) and loaded onto a vacuum liquid chromatography (VLC) column (10 × 8 cm; 15–40 μm silica gel, Merck, Darmstadt, Germany), which was eluted with heptane and then a gradient of heptane–EtOAc (100:1–15:1). The fractions strongly enriched in (2RS, 3SR)- and (2RS, 3RS)-stereoisomers (**1a** and **2a**), respectively, were re-chromatographed, and upon crystallization (EtOH) of the resulting almost pure fractions, crystalline **1a** (4.09 g, 41%; TLC: R_f 0.16 in heptane–EtOAc 15:1) and crystalline **2a** (1.01 g, 10%; TLC: R_f 0.13 in heptane–EtOAc 15:1) were obtained.

2.2.2. Corynomycolic acid ***1b***

The ester **1a** (3.91 g; 7.65 mmol) was dissolved in EtOH (80 ml) and heated in an oil bath (75 °C), while hot 5% aq. KOH (57 ml) was added. Upon continued heating for 3.5 h under vigorous stirring, the reaction mixture was allowed to reach room temperature and was then diluted with water (40 ml). The mixture was acidified with 4 M HCl (3–4 ml; pH < 6), and then $CHCl_3$ (200 ml) was added. The aqueous phase was extracted with additional $CHCl_3$ (200 ml); the combined organic phases were washed with water (200 ml), dried (Na_2SO_4), and concentrated to give a crude product (3.29 g) which was crystallized (EtOH) to give pure hydroxy acid **1b** (3.19 g, 84%).

2.2.3. Formation of ester ***1c***

To the hydroxy acid **1b** (705 mg, 1.42 mmol) and HOAt (193 mg, 1.42 mmol) in a 100-ml flask was added (*S*)-2,3-isopropylideneglycerol (352 μl, 2.84 mmol) and a solution of 4-(N,N-dimethylamino)pyridine (DMAP, 173 mg, 1.42 mmol) in dry CH_2Cl_2 (30 ml). Then, dicyclohexylcarbodiimide (DCC, 439 mg, 2.13 mmol) in dry CH_2Cl_2 (10 ml) was added. After stirring for 15 min, additional (*S*)-2,3-isopropylideneglycerol (352 μl, 2.84 mmol) was added, and then the mixture was stirred for 16 h. The reaction mixture was concentrated *in vacuo*, and the residue was dissolved in CH_2Cl_2 (8 ml) and loaded onto a VLC column (6 × 4 cm; 15–40 μm silica gel). Elution with heptane and then heptane–EtOAc (25:1 and 20:1) afforded the ester **1c** (535 mg, 62%; TLC: R_f 0.25 in heptane–EtOAc 5:1).

2.2.4. Hydrolysis of acetonide

Ester **1c** (232 mg) was hydrolyzed in TFA–THF–H_2O (8:17:3, 14 ml) for 3.5 h at room temperature. The reaction mixture was diluted with CH_2Cl_2 (200 ml) and was then neutralized with saturated aqueous $NaHCO_3$ (ca. 100 ml). The organic layer was washed with water and brine (each 100 ml), dried (Na_2SO_4), and concentrated. The residue was dissolved in CH_2Cl_2 (10 ml) and loaded onto a VLC column (6 × 4 cm; 15–40 μm silica gel). Elution with heptane and then heptane–EtOAc 25:1 to 2:1 gave MMG-**1** (176 mg, 81%; TLC: R_f 0.22 in heptane–EtOAc 3:2).

2.3. Preparation of liposomes by the thin film method

DDA and DDA/MMG-**1** liposomes were prepared by the thin film method essentially as described previously [9]. Briefly, weighed amounts of DDA and MMG-**1** were dissolved in $CHCl_3$–MeOH (9:1), and then the organic solvent was evaporated under vacuum resulting in a thin lipid film. The film was stripped twice with EtOH and dried overnight to remove trace amounts of the solvents. The lipid film was rehydrated by adding Tris buffer (10 mM, pH 7.4) and heating at 60 °C for 1 h with vortex mixing every tenth minute. The final concentrations of DDA and MMG-**1** were 2.5 mg/ml and 0–1.0 mg/ml, respectively.

2.4. Size, polydispersity, and zeta-potential

The average particle size distribution and polydispersity index (PDI) of the liposomes were determined by dynamic light scattering using the photon correlation spectroscopy (PCS) technique. The surface charge of the particles was estimated by analysis of the zeta-potential (laser-Doppler electrophoresis). For determination of the size distribution and PDI, six measurements were performed on samples diluted 10-fold in 10 mM Tris buffer (n = 3). For evaluation of the zeta-potential, three measurements were performed on samples diluted 300-fold in Tris buffer (n = 3). Both types of measurements were performed at 25 °C using a Zetasizer Nano ZS (Malvern Instruments, Worcestershire, UK) equipped with a 633-nm laser and 173° detection optics. Malvern DTS v.5.10 software (Malvern Instruments, Worcestershire, UK) was used for data acquisition and analysis. For viscosity and refractive index, the values of pure water were used. The particle size distribution is reflected in the PDI, which ranges from 0 for a monodisperse to 1.0 for an entirely heterodisperse dispersion.

2.5. Liposome stability

For stability studies, undiluted liposomes (n = 3) were stored in 10 mM Tris buffer with 1 mM NaN_3 at 4 °C or 25 °C for up to 6 months. The particle size was measured at regular intervals as described previously.

2.6. Cryo-TEM

Morphological analysis was carried out by cryo-transmission electron microscopy (cryo-TEM) using a Philips CM120 BioTWIN transmission electron microscope (Philips, Eindhoven, Holland). Samples for cryo-TEM were prepared under controlled temperature and humidity conditions within an environmental verification system. A small droplet (5 μl) of sample was deposited onto a Pelco Lacey carbon-filmed grid. The droplet was spread carefully and excess liquid was removed with a filter paper, resulting in the formation of a thin (10–500 nm) sample film. Then, the samples were immediately plunged into liquid ethane at −180 °C. The vitrified samples were subsequently transferred in liquid nitrogen to an Oxford CT 3500 cryo holder connected to the electron microscope. The sample temperature was continuously kept below −180 °C. All observations were made in the bright field mode at an acceleration voltage of 120 kV. Digital pictures were recorded with a Gatan Imaging Filter 100 CCD camera (Gatan, Pleasanton, CA, USA).

2.7. Differential scanning calorimetry

The gel-to-liquid crystalline phase transition temperature of the undiluted vesicles in suspension was determined by differential scanning calorimetry (DSC). Thermograms were obtained with a Nano DSC (TA Instruments, New Castle, DE, USA) at a scanning rate of 0.5 °C/min in the temperature range from 20 °C to 60 °C. Origin® 7 scientific plotting software was used for data analysis. The first of three scans of each sample (n = 3) was used for data analysis.

2.8. Langmuir–Blodgett isotherms

Surfactant monolayers were formed at room temperature by spreading a total amount of 27.7 nmol lipid mixture of DDA and MMG-**1** (containing 0, 4, 18, 31, or 100 mol% MMG-**1**, respectively) in $CHCl_3$–MeOH (9:1) on an aqueous subphase in a KSV Minitrough

1 (KSV Instruments Ltd., Helsinki, Finland) using a Hamilton microsyringe. The aqueous subphase consisted of 10 mM Tris buffer (pH = 7.4). The compression of the monolayer was initiated 10 min after spreading the lipids to allow the organic solvent to evaporate. The monolayer was compressed with a barrier speed of 10 mm/min, and the surface pressure/area isotherm was detected using a Wilhelmy platinum plate (KSV Instruments Ltd.). Each sample ($n = 3$) was compressed once. KSV software (KSV Instruments Ltd.) was used for data analysis.

2.9. Animal experiments

Female C57BL/6 mice were purchased from Harlan (Horst, The Netherlands). The mice were allowed free access to water and food, and they were 8–10 weeks old at experiment initiation. The protocol for the animal experiments was approved by the Danish Council for Animal Experiments and carried out in accordance with European Community Directive 86/609. Before injection, the vaccines were prepared as follows: A dose of 2 μg recombinant Ag85B-ESAT-6 (Statens Serum Institut, Denmark [13]) and the different adjuvant formulations were mixed in 10 mM Tris buffer and left at room temperature for 30 min with intermittent mixing to allow for proper surface adsorption of the antigen to the liposomes. The amount of DDA was 250 μg/dose, and the MMG-**1** amount was varied from 0 to 150 μg/dose. The mice ($n = 5$) were immunized subcutaneously with 200 μl of vaccine three times at 2-week intervals. Three weeks after the final immunization, the mice were sacrificed, and single-cell suspensions of spleen cells were obtained by passage of spleens through a metal mesh followed by two washings with RPMI 1640 (Gibco Invitrogen, Carlsbad, CA, USA). The cell suspensions were subsequently cultured in RPMI 1640 (GIBCO Invitrogen) supplemented with 10% (v/v) heat-inactivated fetal bovine serum, 5×10^{-6} M β-mercaptoethanol, 1% (v/v) penicillin–streptomycin, 1% (v/v) sodium pyruvate, 1 mM L-glutamine, and 10 mM HEPES in round-bottomed 96-well plates at a density of 2×10^5 cells/well. The cells were re-stimulated with 5 μg/ml Ag85B-ESAT-6. Wells containing medium alone or 5 μg/ml of concanavalin A (Sigma–Aldrich, St. Louis, MO, USA) were included as negative and positive controls, respectively. After 3 days, the supernatants were collected and interferon (IFN)-γ, interleukin (IL)-17, and IL-5 production was quantified by a standard enzyme-linked immunosorbent assay (ELISA) protocol. Briefly, purified rat α-mouse IFN-γ or IL-17 (BD Biosciences, San Jose, CA, USA) was used as capture and biotin-conjugated rat α-mouse IFN-γ or IL-17 (BD Biosciences) was used as detection antibodies, respectively, followed by horse-radish peroxidase (HRP)-conjugated streptavidin (BD Biosciences) and TMB (3,3′,5,5′-tetramethylbenzidine) Plus Ready-to-use substrate (Kem-En-Tec, Taastrup, Denmark). The reaction was stopped at the optimal color development with 0.2 M H_2SO_4, and absorbance was read at 450 nm with wavelength correction at 570 nm to correct for optical imperfections in the plates including air bubbles. The IL-5 production was measured by the OptEIA Mouse IL-5 Set according to the manufacturer's instructions (BD Biosciences). Three weeks after the third immunization, the frequency of IL-4 producing cells was measured by the Mouse IL-4 ELISPOT Set (BD Biosciences) according to the manufacturer's instructions after stimulation of 2×10^5 splenocytes/well with 5 μg/ml of the vaccine antigen overnight. Detection of antibodies in the sera from the immunized mice was done by ELISA: 96-well MaxiSorp plates (Nunc, Denmark) were coated with 0.5 μg/ml Ag85B-ESAT-6 antigen in 15 mM Na_2CO_3, 35 mM $NaHCO_3$ (pH 9.7) overnight at 4 °C. The plates were blocked with PBS containing 2% BSA (w/v), and the sera from the individual mice were added in serial dilutions in a concentration range covering both the maximum and minimum plateau levels. Antigen-specific antibodies were detected with rabbit α-mouse IgG1 or IgG2c conjugated to HRP (Zymed/Invitrogen, Denmark) using TMB Plus Ready-to-use as substrate. The reaction was stopped at the optimal color development with 0.2 M H_2SO_4, and absorbance was read at 450 nm with wavelength correction at 570 nm. Antibody midpoint titers were determined, using the Graphpad Prism 5.03 software, as the reciprocal dilution giving an OD of 50% of the maximal OD value. The detection limit was a midpoint titer of 1000.

2.10. Statistics

Statistical analyses were done by one-way ANOVA at a 0.05 significance level followed by Tukeys posttest using GraphPad Prism (GraphPad Software, La Jolla, CA, USA) unless otherwise stated. Differences in cytokine and antibody levels between different animal groups were compared statistically by one-way ANOVA followed by Dunnett's multiple comparison test.

3. Results

3.1. Synthesis of MMG-*1*

The stereoisomeric MMG analogue, MMG-**1**, based on a synthetic corynomycolic acid isomer was prepared by using a modification of a previously reported pathway [18–20] (Fig. 1B). MMG-**1** consists of a mixture of two diastereomers with (2*R*, 3*S*, 2′*R*)- and (2*S*, 3*R*, 2′*R*) configuration, respectively (Fig. 1B, MMG-**1**). The corresponding racemic methyl ester (Fig. 1B-1a) was obtained as the major isomer from reduction of the keto ester resulting from Claisen condensation of methyl palmitate [21]. The present modifications included substitution of the traditional eluent chloroform with less toxic heptane–ethyl acetate mixtures which also gave more reproducible separations. The purification method was changed to VLC that allows more readily for large-scale separations using less column material and solvents. Furthermore, employing the previously reported [18,20] DCC/4-pyrrolidinopyridine procedure for the ester formation between (*2*RS, *3*SR)-mycolic acid (Fig. 1B-1b) and (*S*)-isopropylidene-glycerol resulted in an undesired dimeric by-product (without a glycerol moiety) being predominant over the expected glycerol ester. To overcome this, several other methods for esterifications [22,23] including forced conditions usually employed for peptide couplings [24,25] were considered. It was found that DCC/HOAt/DMAP [24] constitutes conditions that afford reproducible yields (approx. 60–65%) of the 1,2-isopropylidene-protected MMG ester (Fig. 1B-1c). Also, the yield of the final hydrolysis of the protected MMG ester to MMG-**1** (Fig. 1B, v) was found to be markedly higher when the reaction time was limited to 3–4 h instead of proceeding overnight. A careful NMR spectroscopic characterization revealed that it is possible to distinguish the two diastereomers with (2*R*, 3*S*, 2′*R*)- and (2*S*, 3*R*, 2′*R*) configuration, respectively. The chemical shifts of the signals corresponding to the polar head group and the adjacent part of the lipid moiety differed only slightly indicating that the glycerol moiety and the lipid part do not interact (e.g. by hydrogen bond formation) in a way that determines the overall conformation. In conclusion, the present modifications have improved the overall yield and should readily allow for an upscaling to gram amounts.

3.2. Binary mixtures of DDA and MMG-*1* form liposomes upon dispersion in aqueous media

MMG-**1** was incorporated into the bilayer of DDA liposomes by the thin film method at three different molar ratios (4, 18, and 31 mol%), corresponding to DDA:MMG-**1** weight ratios of 5:0.2, 5:1, and 5:2, respectively. At MMG-**1** contents of 40 mol% and

above, the lipid films could not be fully rehydrated at the applied experimental conditions. This indicates that DDA serves as a solubility enhancer that keeps the MMG-**1** lipid in dispersion by inclusion into the liposomal bilayer, and that MMG-**1** cannot be fully solubilized at high MMG-**1** to DDA molar ratios. The physicochemical characteristics of the resulting DDA and DDA/MMG-**1** liposomes were studied by dynamic light scattering, laser-Doppler electrophoresis, and cryo-TEM. The values for the average particle size, PDI, and zeta-potential of the DDA liposomes with varying content of MMG-**1** are given in Table 1. The average particle diameter of DDA liposomes was around 400 nm as reported previously [9], and the incorporation of MMG-**1** into the DDA liposomes did not change the particle size significantly, irrespectively of the MMG-**1** content. The zeta-potential can affect the particle stability, and it may be used as a measure of the particle surface charge. Thus, DDA liposomes had a high positive surface charge corresponding to a zeta-potential of approximately +70 mV (Table 1). Incorporation of the neutral MMG-**1** did not alter the zeta-potential significantly at any of the tested concentrations. Importantly, the cryo-TEM micrographs confirmed that liposomes were formed when MMG-**1** was incorporated into DDA liposomes (Fig. 2A). As evident from the PDI values (0.4–0.5), the liposome suspensions were rather polydisperse displaying a broad and bi-modal particle size distribution (Fig. 2B). Two main particle populations were apparent from the particle size distribution diagrams and on the cryo-TEM images: One population consisted of faceted, small unilamellar vesicles with particle sizes around 100 nm (Fig. 2A), whereas the second population was large liposomes in the micrometer range and some of these appeared multilamellar (Fig. 2A). Published cryo-TEM micrographs of DDA liposomes support that the vesicles may adopt a faceted morphology [26,27]. However, the origin of these irregular structures has not yet been fully elucidated but could be related to the high bending rigidity of the DDA bilayers [28].

Table 1
Particle size, PDI, and zeta-potential of DDA liposomes with different amounts of MMG-**1** incorporated (mean ± SD, $n = 3$).

Mol% MMG-1	*z*-Average (nm)	PDI	Zeta-potential (mV)
0	422 ± 42	0.51 ± 0.01	72.2 ± 5.2
4	453 ± 36	0.43 ± 0.13	79.2 ± 6.6
18	457 ± 15	0.39 ± 0.01	69.0 ± 1.3
31	333 ± 90	0.42 ± 0.04	72.1 ± 2.4

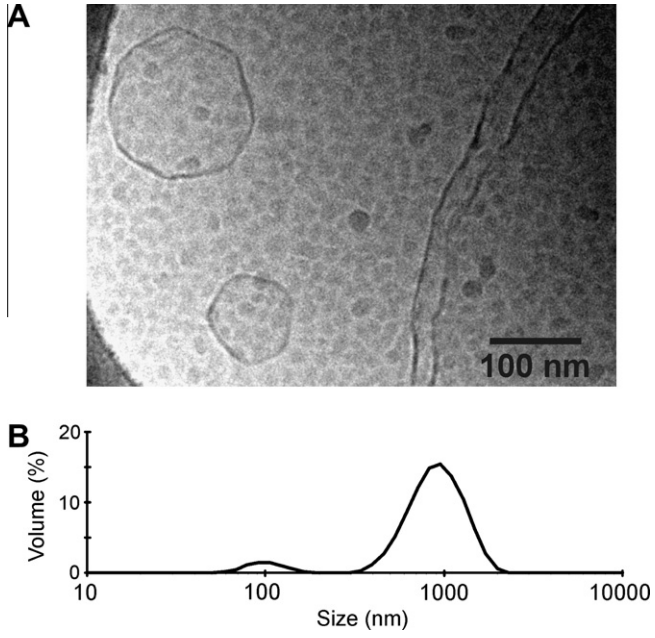

Fig. 2. (A) Cryo-TEM micrograph of DDA/MMG-**1** liposomes with 18 mol% MMG-**1** incorporated into the bilayer. (B) A representative volume-based particle size distribution of DDA/MMG-**1** liposomes with 18 mol% MMG-**1**.

3.3. MMG-*1* stabilizes DDA liposomes

DDA liposomes are physically unstable in suspension and aggregate during prolonged storage [9]. It was thus investigated whether the incorporation of MMG-**1** into the bilayer of DDA liposomes would provide a stabilizing effect. The colloidal stability of DDA liposomes with 0, 4, 18, or 31 mol% MMG-**1** was evaluated during storage for 6 months at 4 and 25 °C, respectively. The average particle size of pure DDA liposomes increased as expected during the first weeks of storage at 4 °C, and visible aggregates were formed (Fig. 3A). Likewise, the liposomes containing 4 mol% MMG-**1** exhibited an increase in particle size during storage at 4 °C, whereas the particle size of liposomes with 18 or 31 mol% MMG-**1**, respectively, was preserved upon storage for 6 months at 4 °C (Fig. 3A), indicating that incorporation of MMG-**1** into DDA liposomal bilayers confers long-term stability to the liposomes at the applied experimental conditions. Similar results were obtained at room temperature (25 °C) since DDA liposomes with 18 or 31 mol% MMG-**1** were stable for 6 months, whereas pure DDA liposomes or DDA liposomes with 4 mol% MMG-**1** showed a

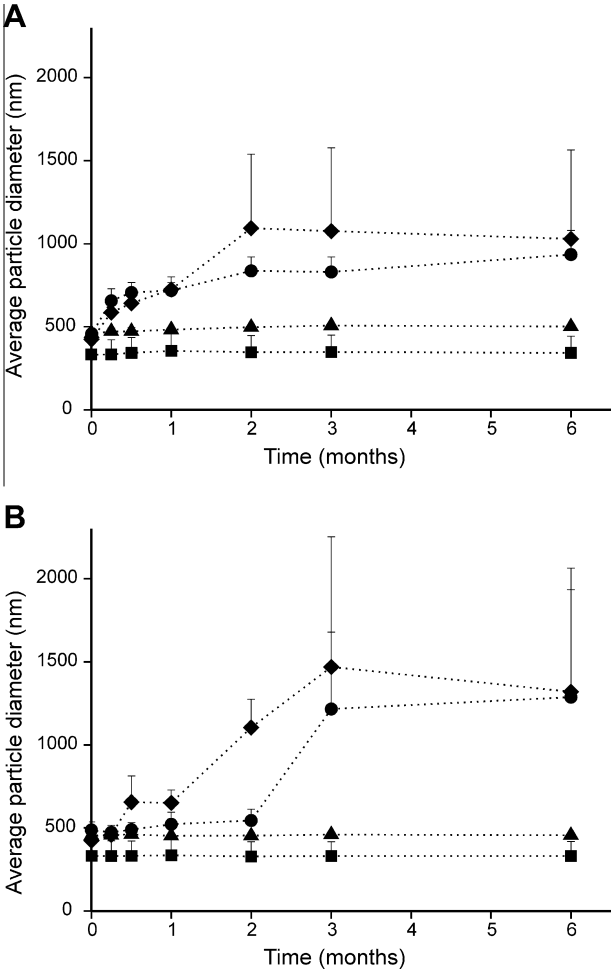

Fig. 3. Average particle size (*z*-average) of DDA liposomes (♦) containing 4 (●), 18 (▲), and 31 mol% (■) MMG-**1** stored at 4 °C (A) or 25 °C (B) as an indication of colloidal stability upon storage. Results denote the means + SD of three batches.

marked increase in particle size (Fig. 3B). Major changes in the surface charge were not detected with the applied methods since the zeta-potential of the colloidally stable formulations remained constant during the 6-month period (results not shown).

3.4. Incorporation of MMG-**1** reduces the phase transition temperature of DDA liposomes

The thermotropic phase behavior of DDA/MMG-**1** liposomes was characterized by differential scanning calorimetry (DSC) to further elucidate how the incorporation of MMG-**1** affected the thermodynamic properties of the membrane. Membrane bilayers undergo a transition from a gel phase to a liquid crystalline phase at the main phase transition temperature (T_m). DSC thermograms for DDA liposome suspensions containing increasing amounts of MMG-**1** are shown in Fig. 4, and the thermodynamic parameters T_m, the width of the phase transition peak at half height ($T_{½}$), and the phase transition enthalpy (ΔH) are summarized in Table 2. The T_m of liposomes composed of pure DDA was approximately 46.6 °C which is in accordance with literature data [9,11,29–32]. The sharpness of the peak ($T_{½}$ = 0.6 °C) suggests a highly cooperative gel-to-fluid phase transition in which the majority of the lipid membrane molecules undergoes a simultaneous phase transition. In general, incorporation of MMG-**1** decreased the T_m, confirming that MMG-**1** is actually incorporated into the bilayer and affects the packing of the DDA molecules in the membrane. Incorporation of 4 mol% MMG-**1** broadened the phase transition peak ($T_{½}$ = 1.5 °C) displaying two interconnected peaks with the main peak at 45.8 °C and a smaller peak at 41.9 °C. This suggests that the lipids are not homogenously distributed, resulting in a phase separation phenomenon characterized by the formation of local membrane microstructures enriched in either DDA or MMG-**1**. Interestingly, incorporation of 18 mol% MMG-**1** resulted in a sharp phase transition peak ($T_{½}$ = 0.6 °C) similar to that of DDA but at a significantly lower temperature (41.5 °C). This sharp phase transition peak suggests a uniform distribution of MMG-**1** in the lipid membrane at this molar ratio. By contrast, incorporation of 31 mol% MMG-**1** into DDA liposomes resulted in a broader phase transition exhibiting two interconnected peaks with the main peak at 41.7 °C and a smaller peak at 47.6 °C. Thus, the main peak was observed at the same temperature as the phase transition of DDA liposomes with 18 mol% MMG-**1**. The phase transition enthalpy of DDA liposomes remained constant after incorporation of 4 and 18 mol% MMG-**1** but was slightly decreased after incorporation of 31 mol% MMG-**1**.

Table 2
Thermodynamic properties of DDA liposomes with different amounts of MMG-**1** incorporated (mean ± SD, n = 3).

Mol% MMG-1	T_m (°C)	$T½$ (°C)	ΔH (kJ/mol)
0	46.6 ± 0.1	0.60 ± 0.11	33.1 ± 1.8
4	45.8 ± 0.2**	1.47 ± 0.17***	36.1 ± 1.8
18	41.5 ± 0.2***	0.55 ± 0.04	33.3 ± 2.6
31	41.7 ± 0.1***	0.81 ± 0.01	27.0 ± 2.2*

* $p < 0.05$, compared to 0 mol% MMG-**1**
** $p < 0.01$, compared to 0 mol% MMG-**1**
*** $p < 0.001$, compared to 0 mol% MMG-**1**.

3.5. Incorporation of MMG-**1** increases the hydration and improves packing of the DDA monolayer

The effects of the MMG-**1** content on the packing and surface pressure of DDA liposomes were investigated further by analyzing Langmuir–Blodgett monolayers of DDA in the presence of different concentrations of MMG-**1**. The results are shown in Fig. 5, and the values for the surface pressure (Π) and the mean molecular area (A) at the monolayer collapse and at the phase transition from the liquid-expanded to the liquid-condensed phase are listed in Table 3. Monolayers of pure DDA collapsed at a mean molecular area of 45.0 Å^2/molecule and a surface pressure of 46.8 mN/m (Fig. 5, arrow 1) as reported previously for DDA on aqueous subphases [11,33]. For the monolayer containing 4 mol% MMG-**1**, the collapse characteristics were similar to pure DDA monolayers. Likewise, the surface pressure at the collapse of the monolayer containing 18 mol% MMG-**1** was also unaffected, whereas the mean molecular area at the collapse was decreased to 41.1 Å^2/molecule, suggesting an improved packing of the lipid molecules. With a content of 31 mol% MMG-**1** in the monolayer, the collapse occurred at a significantly higher surface pressure (59.9 mN/m) and a lower area (33.7 Å^2/molecule) (Fig. 5, arrow 2), indicating that this composition results in a much more stabilized monolayer in which the lipids are packed even more densely. The improved packing may be explained by a decreased repulsion between the positively charged quaternary ammonium head groups of DDA due to the presence of the neutral head groups of the MMG-**1** molecules that intercalate between the DDA molecules. Interestingly, the surface pressure at the collapse of both pure MMG-**1** and pure DDA monolayers was

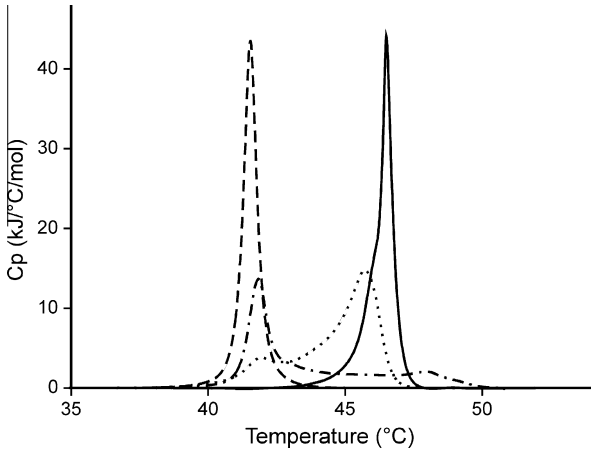

Fig. 4. Differential scanning heat capacity curves for DDA liposomes (solid) containing 4 (dot), 18 (dash), and 31 mol% MMG-**1** (dash-dot). The curves have been normalized to the molar content. The curves represent averages of three experiments for each type of formulation.

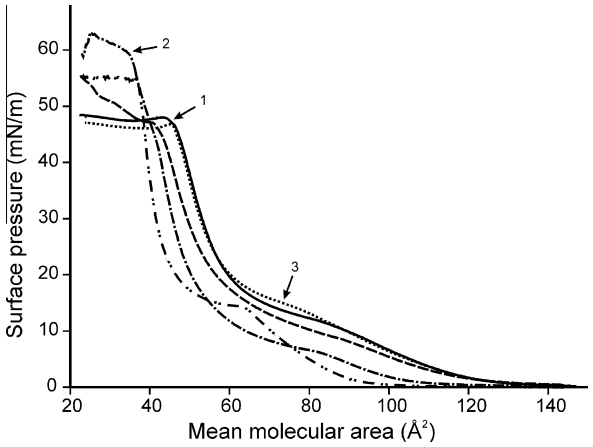

Fig. 5. Pressure/area isotherms of Langmuir–Blodgett monolayers of DDA (solid) with 4 (dot), 18 (dash), 31 (dash-dot), and 100 mol% MMG-**1** (dash-dot-dot) on 10 mM Tris buffer subphases. The total molar lipid concentration of the different monolayers is identical for all experiments. The curves represent averages of three experiments. Arrows: (1) Collapse of DDA monolayer. (2) Collapse of DDA/MMG-**1** monolayer with 31 mol% MMG-**1**. (3) Phase transition of DDA monolayer.

Table 3
Surface pressure (Π) and mean molecular area (A) for DDA/MMG-**1** monolayers (mean ± SD, n = 3).

Mol% MMG-1	Collapse		Phase transition	
	Π (mN/m)	*A* (Å^2)	*Π* (mN/m)	*A* (Å^2)
0	46.8 ± 0.1	45.0 ± 0.9	15.0 ± 0.2	73.1 ± 1.4
4	47.5 ± 0.4	45.3 ± 1.1	13.0 ± 0.1***	76.2 ± 0.9
18	47.0 ± 0.2	41.1 ± 1.3**	8.5 ± 0.0***	88.6 ± 3.6***
31	59.9 ± 0.5***	33.7 ± 1.1***	6.6 ± 0.7***	79.5 ± 2.5*
100	54.7 ± 0.5***	37.1 ± 0.7***	14.4 ± 0.3	63.6 ± 1.1**

* $p < 0.05$, compared to 0 mol% MMG-**1**
** $p < 0.01$, compared to 0 mol% MMG-**1**
*** $p < 0.001$, compared to 0 mol% MMG-**1**.

lower when compared to DDA monolayers with 31 mol% MMG-**1**, suggesting an enhanced stabilization of monolayers containing DDA and MMG-**1** at specific ratios. Monolayers composed of DDA exhibited a transition from liquid-expanded to liquid-condensed phase at a mean molecular area of 73.1 Å^2/molecule and a surface pressure of 15.0 mN/m (Fig. 5, arrow 3). The phase transition was also affected by the presence of MMG-**1** in the monolayer and in general, the phase transition appeared at a lower surface pressure and a higher mean molecular area for binary mixtures of DDA and MMG-**1**.

3.6. Incorporation of MMG-*1* enhances adjuvant efficacy

The adjuvant efficacy of the different formulations of MMG-**1** incorporated into DDA liposomes was also investigated. Mice were immunized subcutaneously three times with the tuberculosis fusion protein Ag85B-ESAT-6 mixed with DDA liposomes containing increasing amounts of MMG-**1** (0, 4, 18, 31, and 40 mol% corresponding to murine doses of 0, 10, 50, 100, and 150 μg MMG-**1**, respectively). The Ag85B-ESAT-6 antigen has a theoretical pI value of 4.80 and is therefore negatively charged at physiological pH; thus, the majority of antigen is expected to adsorb to the cationic DDA-based liposomes via electrostatic interactions [9]. The formulation with 40 mol% MMG-**1** was included in the immunization experiments to investigate if increasing the MMG-**1** dose could further enhance the immune response despite suboptimal liposome characteristics. The T-cell-mediated immune response was assessed 3 weeks after the last immunization. Stimulation of spleen cells with Ag85B-ESAT-6 *in vitro* for 3 days showed that MMG-**1** significantly enhanced the secretion of the Th1 cytokine IFN-γ (Fig. 6A) and the Th17 cytokine IL-17 (Fig. 6B), but not the Th2-associated cytokine IL-5 (Fig. 6C). Incorporation of 31–40 mol% MMG-**1** resulted in significantly increased IFN-γ responses compared to the group that received antigen mixed with DDA. For IL-17, only the formulation containing 31 mol% MMG-**1** induced a significant increase. The production of the classical Th2-associated cytokine IL-4 was investigated by an ELISPOT assay to determine the frequency of IL-4 producing cells since IL-4 levels are notoriously difficult to determine in cell culture supernatants by ELISA due to rapid uptake by IL-4 receptor-expressing cells (Fig. 6D). As observed for IL-5 secretion, a low frequency was observed which was independent of the concentration of MMG-**1**. The data support previous findings that MMG-**1** is a Th1 immunopotentiator [19]. Furthermore, it was found that 31 mol% MMG-**1** also induced a highly significant Th17 response. Thus, the optimal dose of MMG-**1** found for the induction of high Th1/Th17 responses in this DDA-based adjuvant system was 31 mol%.

3.7. Incorporation of 31 mol% MMG-*1* increases IgG2c antibody titers

Since Th1 responses are commonly associated with a relative increase in the levels of antibodies of the IgG2a/IgG2c isotype

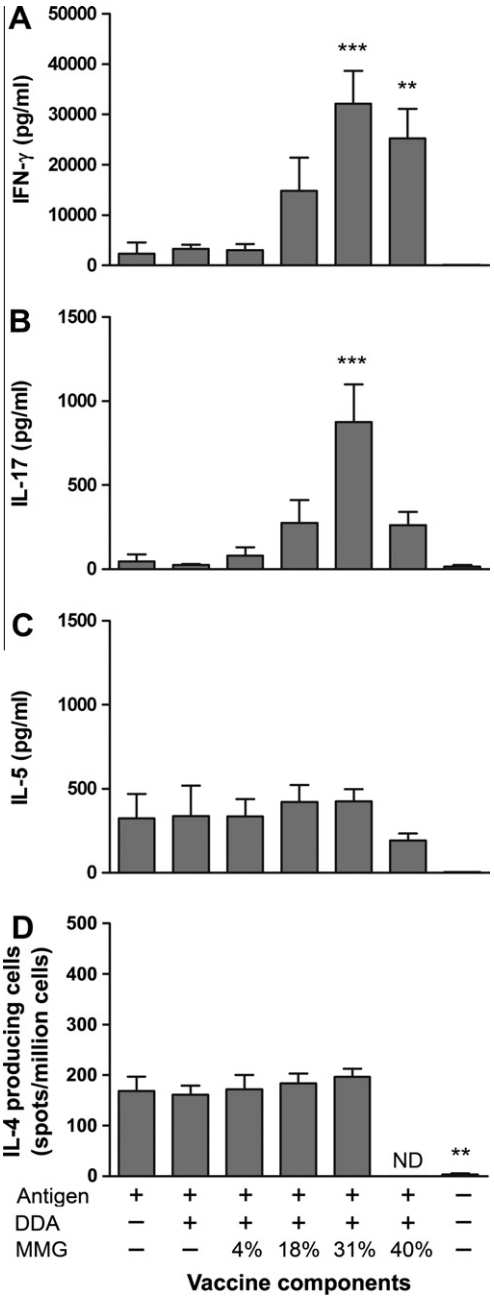

Fig. 6. Production of the cytokines IFN-γ (A), IL-17 (B), and IL-5 (C) by re-stimulated splenocytes isolated from C57BL/6 mice immunized with 2 μg of Ag85B-ESAT-6 and DDA liposomes with 0, 4, 18, 31, or 40 mol% MMG-**1** incorporated, respectively. Three weeks after the third immunization, splenocytes from individual mice were re-stimulated with 5 μg/ml of the antigen for 72 h *in vitro* and cytokine release was measured by ELISA. A similar analysis of the frequency of IL-4 producing splenocytes was done by ELISPOT (D). Bars denote mean cytokine levels, and error bars denote SEM ($n = 5$). Responses significantly different from the antigen/DDA group are indicated: $p < 0.05^{*}$, $p < 0.01^{**}$, and $p < 0.001^{***}$. The cytokine release data shown are representative for two experiments yielding similar results. ND (not done).

compared to IgG1, the antibody midpoint titers were measured in sera from the mice 3 weeks after the last immunization (Fig. 7). In general, all formulations induced robust antibody titers of the readily induced IgG1 isotype (Fig. 7A) irrespective of the concentration of MMG-**1**. However, in accordance with the cytokine data, the level of the Th1-associated IgG2c isotype, which is the IgG2a equivalent expressed in C57BL/6 mice, was significantly increased only when 31 mol% MMG-**1** was incorporated (Fig. 7B).

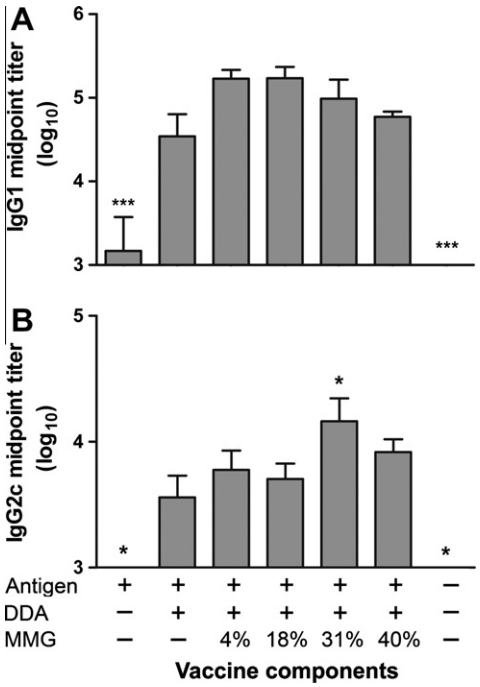

Fig. 7. Circulating antibodies of the IgG1 (A) and IgG2c (B) isotypes in blood from C57BL/6 mice immunized with 2 μg of Ag85B-ESAT-6 and DDA liposomes with 0, 4, 18, 31, or 40 mol% MMG-**1** incorporated, respectively. Blood samples were drawn 3 weeks after the third immunization, and the antibody levels in the serum of each individual mouse were determined as midpoint titers by ELISA. The detection limit was a dilution factor of 1000. Bars denote mean midpoint titers, and error bars denote SEM ($n = 5$). Responses significantly different from the antigen/DDA group are indicated: $p < 0.05^{*}$, $p < 0.01^{**}$, and $p < 0.001^{***}$. The data shown are representative for two experiments yielding similar results.

4. Discussion

The combination of delivery systems and immunopotentiators represents an attractive strategy for customizing adjuvants toward a given immunological profile. Whereas delivery systems in general ensure the delivery of antigens to antigen-presenting cells (APCs), immunopotentiators activate immune cells, commonly through specific receptors and/or intracellular signaling pathways. However, some delivery systems may also have intrinsic immunopotentiating properties [34,35]. The cationic charge of DDA liposomes enables effective interaction with antigens with pI values below physiological pH as well as with the negatively charged heparane sulfate proteoglycans present on the surface of APCs. Previous studies show that one adjuvant mechanism of DDA liposomes is to bind to the cell membrane of APCs via electrostatic interactions resulting in enhanced uptake and presentation of liposome-associated antigens [36]. The potential of DDA-based liposomal adjuvants has been evaluated in different experimental vaccines against viruses [6,37] as well as bacteria [4]. Incorporating MMG-**1** into the lipid bilayer of DDA liposomes may further potentiate the adjuvant effect.

In the present study, incorporation of MMG-**1** into DDA liposomes potentiated an antigen-specific Th1/Th17 immune response in a dose-dependent manner with maximal effect at 31 mol% MMG-**1**. It has previously been suggested that synthetic MMG can enhance the immune response at very low concentrations (0.2–4 mol% MMG in DDA liposomes) [18–20]. This is in contrast to the current study which indicates that the presence of more than 18 mol% MMG-**1** in DDA liposomes is required to enhance the immune response. The highest T-cell-mediated immune responses were observed for formulations with 31 mol% MMG-**1**, characterized by high IFN-γ and IL-17 responses. This is most likely a result of enhanced stimulation of the immune system due to the presence of high concentrations of incorporated MMG-**1** readily accessible for stimulation of APCs. At 40 mol% MMG-**1**, the immune response decreased which might be the result of several factors including overstimulation of the immune system and/or reduced liposomal integrity due to the high MMG-**1** to DDA molar ratio. Indeed, it was observed that inclusion of 18–31 mol% MMG-**1** seemed to be optimal with regard to colloidal stability of DDA/MMG-**1** liposomes. At higher MMG-**1** concentrations, the low solubility of MMG-**1** became limiting for the liposome formation process. It was thus observed that inclusion of 40 mol% MMG-**1** or more resulted in incomplete solubilization during the rehydration step at the applied experimental conditions (data not shown).

Lipids of mycobacterial origin have been recognized to possess immunostimulatory activity for many decades. In a recent study, MMG was identified as the most potent compound among several lipids isolated from the mycobacterial cell wall [18,19]. The synthetic analogue based on a C_{32} lipid acid with a stereochemistry corresponding to that present in corynomycolic acid was demonstrated to possess similar activity as the natural compound. In the current study, an MMG analogue based on the more readily accessible palmitate-derived C_{32} lipid acid with a stereochemistry different from natural corynomycolic acid has been investigated. A number of advantages are associated with the use of synthetic analogues. These include a high purity and reproducibility of the final composite adjuvant. Furthermore, the simplified structure of MMG analogues allows for a relatively simple and cheap large-scale chemical synthesis, and formulation of an adjuvant system comprising the immunopotentiator becomes simpler. Another advantage of using a well-defined synthetic compound that retains the immunological activity of the parent compound is that the toxicological profile often is more acceptable when compared to extracted bacterial cell wall components. Examples of these are the different lipid A analogues [38] and TDM analogues [39,40]. Evaluation of the toxicological profile of the MMG lipid and MMG analogues such as MMG-**1** is pending.

Liposomes based on DDA are physically unstable and fuse or aggregate during prolonged storage. Besides potentiating the immune response of DDA, it was shown that incorporation of MMG-**1** effectively stabilizes the DDA liposomes at specific molar ratios. DDA possesses a cationic and relatively small quaternary ammonium head group that exhibits a rather weak interaction with water which may account for the poor colloidal stability of liposomes consisting entirely of DDA. In the Langmuir–Blodgett study, an increased surface pressure is observed in the presence of high concentrations of MMG-**1** when the DDA/MMG-**1** monolayer is fully compressed. This suggests a stronger interaction between the glycerol head group of MMG-**1** and the aqueous subphase than between the quaternary ammonium head group of DDA and the aqueous subphase. Thus, incorporation of MMG-**1** into the lipid bilayer of DDA liposomes might facilitate hydrogen bond formation and lead to increased hydration of the lipid head group region which may account for the improved colloidal stability of the liposomes. This enhanced hydration has also been suggested to account for the stabilizing effect of TDB on DDA liposomes [9,11]. In addition to an increased surface pressure at the fully compressed state, the Langmuir–Blodgett studies also showed a shift in the π–A isotherm to a lower mean molecular area in the presence of MMG-**1**, indicating a more densely packed lipid monolayer, probably reflecting reduced electrostatic repulsion between the DDA head groups.

Besides improved colloidal stability, incorporation of MMG-**1** affected the lipid packing properties as indicated by the analysis of the thermotropic phase behavior. In general, the phase transition temperature was decreased after incorporation of MMG-**1**

which might be due to the shorter chain length of MMG-**1** when compared to DDA since the phase transition temperature typically decreases with decreasing chain length in a liposomal bilayer structure [41,42]. However, in addition to the lipid chain length, the phase transition also depends on other factors such as chain saturation, head group type, head group interactions, van der Waal interactions between the lipid chains as well as the hydration state of the lipid head groups [41,43]. It has been demonstrated that lipid hydration lowers the transition temperature [44,45] which may also explain the decrease in phase transition temperature observed in the presence of MMG-**1** since MMG-**1** enables hydration of the otherwise poorly hydrated DDA bilayer. Thus, several factors may account for the decrease in phase transition temperature observed for the present binary DDA/MMG-**1** system. Although the main phase transition temperature was decreased, T_m is maintained well above 37 °C at all examined DDA/MMG-**1** ratios showing that the liposomes are in the gel-like state at physiological temperatures. This is important as it has previously been demonstrated that the immune response is reduced when the phase transition temperature is systematically decreased by incorporating lipids of shorter chain lengths [46,47]. The heat transition enthalpies remained constant after incorporation of up to 18 mol% MMG-**1**, indicating that the formation of bilayers is dependent on DDA, while MMG-**1** only gives minor contributions to the bilayer phase transition enthalpy which correlated directly to the concentration of DDA. Incorporation of 31 mol% MMG-**1** into the bilayer of DDA liposomes, however, resulted in a slightly decreased heat capacity. Although this did not affect the colloidal stability, it might indicate that the limit for efficient incorporation of MMG-**1** into DDA liposomes is being reached.

Previous results indicate that different structural MMG analogues may possess different immunostimulatory activities [20], suggesting that MMG activates the immune system via a specific receptor-mediated signaling pathway. Thus, we are currently investigating the physical as well as immunological properties of DDA liposomes containing different MMG stereoisomers as well as estimating the effect of altering the lipid chain length of MMG.

5. Conclusion

The present study provides a thorough characterization of DDA/MMG-**1** liposomes and demonstrates that incorporation of MMG-**1** into the bilayer of DDA liposomes increases the stability of the liposomes, most likely in a dual way by enabling hydrogen bond formation between the glycerol moiety of MMG-**1** and the aqueous medium as well as by reducing the head group repulsion between adjacent cationic DDA molecules within the bilayer of the liposomes. In addition, MMG-**1** potentiates the adjuvant efficacy of DDA liposomes, and at the optimal dose, the adjuvant formulation induces a strong Th1/Th17 response as well as a robust antibody response. Thus, DDA liposomes containing 31 mol% MMG-**1** seem to be optimal for providing the most favorable combined physical and immunological properties.

Role of the funding source

This work was funded by the Danish National Advanced Technology Foundation and the Drug Research Academy (PN, EAP, TSK). We acknowledge the Danish Agency for Science, Technology and Innovation for the Zetasizer Nano ZS, the Drug Research Academy for co-funding the KSV Minitrough 1, and The Danish National Advanced Technology Foundation and the Danish Ministry of Science, Technology and Innovation for funding the nano-DSC. Additional funding was provided by the European Commission Grant Agreement No. 241,745. The funding sources had no involvement in the study design; in the collection, analysis, and interpretation of data; in the writing of the report; and in the decision to submit the paper for publication.

Disclosures

Else Marie Agger is co-inventor on a patent covering MMG for use in adjuvant formulations.

Acknowledgements

Thanks to Fabrice Rose, Maja Hauge Nielsen (University of Copenhagen), Julie Folmer Buhelt, and Lama El-Haj (Statens Serum Institut) for excellent technical assistance.

Appendix A. Supplementary material

Supplementary data associated with this article can be found, in the online version, at doi:10.1016/j.ejpb.2010.10.001.

References

[1] B. Guy, The perfect mix: recent progress in adjuvant research, Nat. Rev. Microbiol. 5 (2007) 505–517.
[2] P. Nordly, H.B. Madsen, H.M. Nielsen, C. Foged, Status and future prospects of lipid-based particulate delivery systems as vaccine adjuvants and their combination with immunostimulators, Expert Opin. Drug Deliv. 6 (2009) 657–672.
[3] D. Gall, The adjuvant activity of aliphatic nitrogenous bases, Immunology 11 (1966) 369–386.
[4] E.B. Lindblad, M.J. Elhay, R. Silva, R. Appelberg, P. Andersen, Adjuvant modulation of immune responses to tuberculosis subunit vaccines, Infect. Immun. 65 (1997) 623–629.
[5] L. Brandt, M. Elhay, I. Rosenkrands, E.B. Lindblad, P. Andersen, ESAT-6 subunit vaccination against *Mycobacterium tuberculosis*, Infect. Immun. 68 (2000) 791–795.
[6] C. Klinguer-Hamour, C. Libon, H. Plotnicky-Gilquin, M.C. Bussat, L. Revy, T. Nguyen, J.Y. Bonnefoy, N. Corvaia, A. Beck, DDA adjuvant induces a mixed Th1/Th2 immune response when associated with BBG2Na, a respiratory syncytial virus potential vaccine, Vaccine 20 (2002) 2743–2751.
[7] J.P. Stanfield, D. Gall, P.M. Bracken, Single-dose antenatal tetanus immunisation, Lancet 1 (1973) 215–219.
[8] L.A.T. Hilgers, M.W. Weststrate, Stabilized Adjuvant Suspension Comprising Dimethyldioctadecylammoniumbromide, US 5,026,546, 1991.
[9] J. Davidsen, I. Rosenkrands, D. Christensen, A. Vangala, D. Kirby, Y. Perrie, E.M. Agger, P. Andersen, Characterization of cationic liposomes based on dimethyldioctadecylammonium and synthetic cord factor from *M. tuberculosis* (trehalose 6,6′-dibehenate) – a novel adjuvant inducing both strong CMI and antibody responses, Biochim. Biophys. Acta 1718 (2005) 22–31.
[10] C.N. Sobral, M.A. Soto, A.M. Carmona-Ribeiro, Characterization of DODAB/DPPC vesicles, Chem. Phys. Lipids 152 (2008) 38–45.
[11] D. Christensen, D. Kirby, C. Foged, E.M. Agger, P. Andersen, Y. Perrie, H.M. Nielsen, α,α′-Trehalose 6,6′-dibehenate in non-phospholipid-based liposomes enables direct interaction with trehalose, offering stability during freeze-drying, Biochim. Biophys. Acta 1778 (2008) 1365–1373.
[12] E.M. Agger, I. Rosenkrands, J. Hansen, K. Brahimi, B.S. Vandahl, C. Aagaard, K. Werninghaus, C. Kirschning, R. Lang, D. Christensen, M. Theisen, F. Follmann, P. Andersen, Cationic liposomes formulated with synthetic mycobacterial cordfactor (CAF01): a versatile adjuvant for vaccines with different immunological requirements, PLoS One 3 (2008) e3116.
[13] A.W. Olsen, L.A.H. van Pinxteren, L.M. Okkels, P.B. Rasmussen, P. Andersen, Protection of mice with a tuberculosis subunit vaccine based on a fusion protein of antigen 85B and ESAT-6, Infect. Immun. 69 (2001) 2773–2778.
[14] D. Christensen, E.M. Agger, L.V. Andreasen, D. Kirby, P. Andersen, Y. Perrie, Liposome-based cationic adjuvant formulations (CAF): past, present, and future, J. Liposome Res. 19 (2009) 2–11.
[15] R.E. Geisel, K. Sakamoto, D.G. Russell, E.R. Rhoades, In vivo activity of released cell wall lipids of *Mycobacterium bovis* bacillus Calmette-Guerin is due principally to trehalose mycolates, J. Immunol. 174 (2005) 5007–5015.
[16] G.D. Sprott, C.J. Dicaire, K. Gurnani, S. Sad, L. Krishnan, Activation of dendritic cells by liposomes prepared from phosphatidylinositol mannosides from *Mycobacterium bovis* bacillus Calmette-Guerin and adjuvant activity in vivo, Infect. Immun. 72 (2004) 5235–5246.
[17] I. Rosenkrands, E.M. Agger, A.W. Olsen, K.S. Korsholm, C.S. Andersen, K.T. Jensen, P. Andersen, Cationic liposomes containing mycobacterial lipids: a new powerful Th1 adjuvant system, Infect. Immun. 73 (2005) 5817–5826.
[18] C.S. Andersen, E.M. Agger, I. Rosenkrands, J.M. Gomes, V. Bhowruth, K.J. Gibson, R.V. Petersen, D.E. Minnikin, G.S. Besra, P. Andersen, A simple mycobacterial

monomycolated glycerol lipid has potent immunostimulatory activity, J. Immunol. 182 (2009) 424–432.
[19] C.A. Andersen, I. Rosenkrands, A.W. Olsen, P. Nordly, D. Christensen, R. Lang, C. Kirschning, J.M. Gomes, V. Bhowruth, D.E. Minnikin, G.S. Besra, F. Follmann, P. Andersen, E.M. Agger, Novel generation mycobacterial adjuvant based on liposome-encapsulated monomycoloyl glycerol from *Mycobacterium bovis* bacillus Calmette-Guerin, J. Immunol. 183 (2009) 2294–2302.
[20] V. Bhowruth, D.E. Minnikin, E.M. Agger, P. Andersen, V.W. Bramwell, Y. Perrie, G.S. Besra, Adjuvant properties of a simplified C32 monomycolyl glycerol analogue, Bioorg. Med. Chem. Lett. 19 (2009) 2029–2032.
[21] A.K. Datta, K. Takayama, M.A. Nashed, L. Anderson, An improved synthesis of trehalose 6-mono- and 6,6′-di-corynomycolates and related esters, Carbohydr. Res. 218 (1991) 95–109.
[22] L.J. Goosen, A. Döhring, A convenient protocol for the esterification of carboxylic acids with alcohols in the presence of di-t-butyl dicarbonate, Synlett 2004 (2004) 263–266.
[23] R.T. Pon, S.Y. Yu, Y.S. Sanghvi, Rapid esterification of nucleosides to solid-phase supports for oligonucleotide synthesis using uronium and phosphonium coupling reagents, Bioconjugate Chem. 10 (1999) 1051–1057.
[24] T. Yakura, Y. Yoshimoto, C. Ishida, S. Mabuchi, Synthesis of an immunomodulator (+)-conagenin and its analogs, Tetrahedron 63 (2007) 4429–4438.
[25] A.J. Pearson, M.V. Chelliah, Synthesis of a model bicyclic CDE ring system of ristocetin A and observation of a facile inversion of configuration in a 16-membered DE ring model, J. Org. Chem. 63 (1998) 3087–3098.
[26] E. Feitosa, P.C.A. Barreleiro, The effect of ionic strength on the structural organization of dioctadecyldimethylammonium bromide in aqueous solution, Progr. Colloid Polym. Sci. 128 (2004) 163–168.
[27] E. Feitosa, G. Karlsson, K. Edwards, Unilamellar vesicles obtained by simply mixing dioctadecyldimethylammonium chloride and bromide with water, Chem. Phys. Lipids 140 (2006) 66–74.
[28] M. Kepczynski, J. Bednar, D. Kuzmicz, P. Wydro, M. Nowakowska, Spontaneous formation of densely stacked multilamellar vesicles in dioctadecyldimethylammonium bromide/oleosiloxane mixtures, Langmuir 26 (2010) 1551–1556.
[29] F.M. Linseisen, S. Bayerl, T.M. Bayerl, 2H-NMR and DSC study of DPPC–DODAB mixtures, Chem. Phys. Lipids 83 (1996) 9–23.
[30] M.J. Blandamer, B. Briggs, P.M. Cullis, K.D. Irlam, S.D. Kirby, J.B.F.N. Engberts, Formation of vesicular bilayers in aqueous solutions containing mixtures of dialkyldimethylammonium bromides, J. Mol. Liq. 75 (1998) 181–187.
[31] E. Feitosa, P.C. Barreleiro, G. Olofsson, Phase transition in dioctadecyldimethylammonium bromide and chloride vesicles prepared by different methods, Chem. Phys. Lipids 105 (2000) 201–213.
[32] P.C.A. Barreleiro, G. Olofsson, W. Brown, K. Edwards, N.M. Bonassi, E. Feitosa, Interaction of octaethylene glycol n-dodecyl monoether with dioctadecyldimethylammonium bromide and chloride vesicles, Langmuir 18 (2002) 1024–1029.
[33] A.M. Gonçalves da Silva, M.I. Viseu, Synergism in mixed monolayers of cationic and anionic surfactants: a thermodynamic analysis of miscibility at the air-water interface, Colloids Surf. A. Physicochem. Eng. Asp. 144 (1998) 191–200.
[34] D.T. O'Hagan, E. De Gregorio, The path to a successful vaccine adjuvant – 'the long and winding road', Drug Discov. Today 14 (2009) 541–551.
[35] C. Lonez, M. Vandenbranden, J.M. Ruysschaert, Cationic liposomal lipids: from gene carriers to cell signaling, Prog. Lipid Res. 47 (2008) 340–347.
[36] K.S. Korsholm, E.M. Agger, C. Foged, D. Christensen, J. Dietrich, C.S. Andersen, C. Geisler, P. Andersen, The adjuvant mechanism of cationic dimethyldioctadecylammonium liposomes, Immunology 121 (2007) 216–226.
[37] C.A. Kraaijeveld, G. la Riviere, B.J. Baissa-Trouw, J. Jansen, T. Harmsen, H. Snippe, Effect of the adjuvant dimethyl dioctadecyl ammonium bromide on the humoral and cellular immune responses to encephalomyocarditis virus, Antiviral Res. 3 (1983) 137–149.
[38] J.R. Baldridge, P. McGowan, J.T. Evans, C. Cluff, S. Mossman, D. Johnson, D. Persing, Taking a Toll on human disease: Toll-like receptor 4 agonists as vaccine adjuvants and monotherapeutic agents, Expert Opin. Biol. Ther. 4 (2004) 1129–1138.
[39] G.R. Olds, L. Chedid, E. Lederer, A.A. Mahmoud, Induction of resistance to *Schistosoma mansoni* by natural cord factor and synthetic lower homologues, J. Infect. Dis. 141 (1980) 473–478.
[40] M.V. Pimm, R.W. Baldwin, J. Polonsky, E. Lederer, Immunotherapy of an ascitic rat hepatoma with cord factor (trehalose-6,6′-dimycolate) and synthetic analogues, Int. J. Cancer 24 (1979) 780–785.
[41] G. Cevc, How membrane chain-melting phase-transition temperature is affected by the lipid chain asymmetry and degree of unsaturation: an effective chain-length model, Biochemistry 30 (1991) 7186–7193.
[42] D.A. Mannock, R.N. Lewis, R.N. McElhaney, P.E. Harper, D.C. Turner, S.M. Gruner, An analysis of the relationship between fatty acid composition and the lamellar gel to liquid-crystalline and the lamellar to inverted nonlamellar phase transition temperatures of phosphatidylethanolamines and diacyl-alpha-D-glucosyl glycerols, Eur. Biophys. J. 30 (2001) 537–554.
[43] D. Marsh, General features of phospholipid phase transitions, Chem. Phys. Lipids 57 (1991) 109–120.
[44] G. Cevc, A. Watts, D. Marsh, Titration of the phase transition of phosphatidylserine bilayer membranes. Effects of pH, surface electrostatics, ion binding, and head-group hydration, Biochemistry 20 (1981) 4955–4965.
[45] G. Cevc, Isothermal lipid phase transitions, Chem. Phys. Lipids 57 (1991) 293–307.
[46] O. Bakouche, D. Gerlier, Enhancement of immunogenicity of tumour virus antigen by liposomes: the effect of lipid composition, Immunology 58 (1986) 507–513.
[47] T. Yasuda, G.F. Dancey, S.C. Kinsky, Immunogenicity of liposomal model membranes in mice: dependence on phospholipid composition, Proc. Natl. Acad. Sci. USA 74 (1977) 1234–1236.